10-14 July 2016, Vienna, Austria

Advanced Supported Liquid Membranes for Carbon Dioxide Control in Cabin Applications

David T. Wickham,[1] Kevin J. Gleason,[2] and Jeffrey R. Engel[3]
Reaction Systems, Inc., Golden, Colorado, 80401

and

Cinda Chullen[4]
NASA Johnson Space Center, Houston, Texas, 77058

The development of new, robust, life support systems is critical to NASA's continued progress in space exploration. One vital function is maintaining the carbon dioxide (CO_2) concentration in the cabin at levels that do not impair the health or performance of the crew. The carbon dioxide removal assembly (CDRA) is the current CO_2 control technology on-board the International Space Station (ISS). Although the CDRA has met the needs of the ISS to date, the repeated cycling of the molecular sieve sorbent causes it to break down into small particles that clog filters or generate dust in the cabin. This reduces reliability and increases maintenance requirements. Another approach that has potential advantages over the current system is a membrane that separates CO_2 from air. In this approach, cabin air contacts one side of the membrane while other side of the membrane is maintained at low pressure to create a driving force for CO_2 transport across the membrane. In this application, the primary power requirement is for the pump that creates the low pressure and then pumps the CO_2 to the oxygen recovery system. For such a membrane to be practical, it must have high CO_2 permeation rate and excellent selectivity for CO_2 over air. Unfortunately, conventional gas separation membranes do not have adequate CO_2 permeability and selectivity to meet the needs of this application. However, the required performance could be obtained with a supported liquid membrane (SLM), which consists of a microporous material filled with a liquid that selectively reacts with CO_2 over air. In a recently completed Phase II SBIR project, Reaction Systems, Inc. fabricated an SLM that is very close to meeting permeability and selectivity objectives for use in the Portable Life Support System (PLSS). This paper describes work carried out to evaluate its potential for use in the cabin.

Nomenclature

°C = degrees Celsius
AP-Mim = 1-(3-aminopropyl)-3-methylimidazolium
atm = atmospheres
Btu/h = British thermal units per hour
cc = cubic centimeters
cm^2 = square centimeters
cm-Hg = centimeters of mercury
CO_2 = carbon dioxide
EVA = extravehicular activity
ft^3 = cubic feet

[1] President and Principal Investigator, 17301 W. Colfax Ave, Suite 160, Golden, CO, 80401.
[2] Senior Engineer, 17301 W. Colfax Ave, Suite 160, Golden, CO, 80401.
[3] Senior Engineer, 17301 W. Colfax Ave, Suite 160, Golden, CO, 80401.
[4] Project Engineer, Space Suit and Crew Survival Systems Branch, Crew and Thermal Systems Division, 2101 NASA Parkway/EC5

GC = gas chromatograph
g/h = grams per hour
H_2O = water
h-PTFE = hydrophobic polytetrafluorethyleen
IL = ionic liquid
L = liter
m^2 = square meters
m^3 = cubic meters
mm = millimeters
mmHg = millimeters of mercury
mtorr = millitorr
NMR= nuclear magnetic resonance
O_2 = oxygen
PLSS = portable life support system
P_{tot} = total pressure
RH = relative humidity
s = second
scc = standard cubic centimeters
SLM = supported liquid membrane
slpm = standard liters per minute
T = temperature
μL = microliter
μm = micrometers

I. Introduction

A. Current CO_2 Control Methods

The development of new, robust, lightweight life support systems is currently a crucial need for NASA in order to continue making advances in space exploration. One important area of concern is the control of CO_2 produced by crew in cabin environments. The CDRA, which is the current CO_2 control technology on-board the ISS uses a pressure and temperature swing adsorption cycle to remove carbon dioxide from the crew breathing air[1]. CO_2 is removed with a four-bed molecular sieve (4BMS) system that consists of two desiccant beds and two CO_2 sorbent beds. The CO_2 sorbent beds contain zeolite 5A molecular sieve packed between heater plates. Because water preferentially absorbs and displaces CO_2 on this material, desiccant beds, which consist of silica gel and zeolite 13x molecular sieve, are placed in front of the 5A to dry the incoming flow. The silica gel can adsorb water vapor readily at higher relative humidity (RH) but its capacity falls off at RH less than 50%. The zeolite 13x has a higher capacity than silica gel at RH less than 35% [2].

The operation of the CDRA was described in detail by Murdock [3]. In the current mode of operation, one desiccant bed and one adsorbent bed operate in adsorption mode while the other two beds are being regenerated. Cabin air is drawn through one of the desiccant beds to remove the moisture then directed through one of the CO_2 sorbent beds to remove the CO_2. The dry, CO_2 depleted air is then directed back through the second desiccant bed, which is being heated for regeneration to re-humidify the air stream before returning it back to the cabin. While this is happening, the second CO_2 sorbent bed, which is loaded with CO_2, is heated to 400°F (204°C) and evacuated to 0.5 psia to desorb the CO_2 from the zeolite for storage in the accumulator tank prior to delivery to the Sabatier[2]. The desorption is complete after about 55 min. During daytime operation when power on the ISS is plentiful, heat and vacuum are used to regenerate the CO_2 bed but during nighttime operation, the heaters are turned off [3]. At the start of the next half-cycle, all beds switch to the opposite mode and cabin air flow 'swings' to the other set of adsorbent beds; the alternate bed then performs the CO_2 removal function. In this manner continuous CO_2 removal is achieved.

Although the CDRA has performed well and has reliably controlled CO_2 levels in the ISS for many years, the repeated cycling of the molecular sieve sorbent causes the material to break down into very small particles. The formation of small particles can cause a number of problems, including increasing the pressure drop through the bed, clogging filters, and generating dust in the cabin. These problems require additional maintenance and astronauts valuable time. Therefore, there is a need to find a reliable, low maintenance method for CO_2 control.

B. New Methods for CO_2 Control

Requirements

In addition to eliminating the dusting or filter fouling problem of the CDRA, NASA also intends to reduce the ambient level of CO_2 to 2 mm Hg. Thus, new systems and approaches are under consideration. For a replacement system to be attractive, it should not exceed size, weight, and power specifications of the CDRA system. As shown in Table 1, the volume should be less than 2 ft^3 per crew and the average power consumption including pump efficiencies and heat losses needs to be lower than 118 watts/crew. In addition, the CO_2 flow to the Sabatier reactor must meet several requirements. The flow must be very dry to avoid condensation in the accumulator during the compression cycle and the concentrations of O_2 and N_2 must be less than 1 vol% and 2 vol% respectively.

Table 1. CO_2 Replacement System Guidelines

Parameter	Limit
CO_2 Generation Rate	1 kg/day/crew
CO_2 Concentration	< 2 mm Hg
Volume	< 2 ft^3/crew
Power	< 118 watts/crew
Weight	< 67 lb/crew
Flow toSabatier	
H_2O	DP < -65°C
N_2	< 2 vol%
O_2	< 1 vol%

Use of a Membrane

One approach that could be used for CO_2 control would be a membrane that is selective for CO_2 over O_2 and N_2. An effective membrane would be a simple system with few maintenance issues and no potential to generate dust, which would be a major benefit for the cabin application. In this case, CO_2 would absorb into the membrane from the crew side and be vented on the opposite side where a pump maintains the low pressure needed to generate a driving force. The concentrated CO_2 in the pump effluent could be fed directly and continuously into the oxygen recovery system. This could eliminate the accumulator and compressor, which are required to store CO_2 between regeneration cycles in the CDRA.

However, there are some challenges that must be met for a membrane to be effective. First, it must have a high CO_2 permeation rate to meet the maximum size limitation. We can estimate the permeance requirements using the generation rate, volume, the maximum allowable CO_2 concentration and the surface area to volume ratio expected in a module. In a moderate surface area to volume configuration, a membrane module can contain 50 m^2 of surface area per ft^3 and therefore a module of 2 ft^3 per crew could contain a total surface area of 100 m^2 per crew. A CO_2 generation rate of 1 kg/day per crew is equivalent to 6.44 scc/s per crew, where scc is standard cm^3 at 1 atm and 25°C. Therefore, the flux through the membrane must be 6.4E-6 scc/(cm^2 s). With a maximum driving force of the 2 mm Hg, the permeance must be at least 3.2E-5 scc/(cm^2 s cm Hg). However, as the process flow passes through the module, the CO_2 concentration will decrease but the average flux must remain at 6.4E-6 scc/(cm^2 s). Therefore the permeance should be on the order of 1E-4 scc/(cm^2 s cm Hg). Moreover, the selectivity must be very high to reduce the concentration of N_2 and O_2 in the effluent.

Unfortunately, conventional gas separation membranes do not have an adequate combination of CO_2 permeability and selectivity to meet the needs of either application. However, a supported liquid membrane (SLM) may be a good way to obtain the needed permeance and very high selectivity. SLMs can be extremely effective because they rely on the difference in chemical properties to achieve selectivity for CO_2 over air. In this case, the SLM consists of a porous membrane filled with a reactant that selectively binds the contaminant forming a semi-stable intermediate. The intermediate then diffuses through the liquid in the pores to the low pressure side of the membrane, where the reduced pressure of CO_2 shifts the equilibrium, resulting in the decomposition of the complex and release of the bound CO_2 molecule. In addition, the liquid does not react with N_2 or O_2, which reduces the flow of these gases through the membrane

To achieve selective transport, the liquid reagent material must meet several criteria. First, the affinity between CO_2 and the reagent must be much greater than between N_2 or O_2 and the reagent. Second, the liquid must have low viscosity to allow the complex to diffuse through the pore. Third, the liquid must have extremely low vapor pressure so it does not evaporate when exposed to low presssure. Fortunately, much work has been carried out to develop methods for CO_2 capture and it is therefore well known that CO_2 is an acidic gas and basic compounds such as amines are effective sorbents for CO_2. Unfortunately, since moderate viscosity amines such as diethanolamine are volatile,

they cannot be used in the SLM. Although increasing the molecular weight of the amine by adding functional groups does reduce the vapor pressure somewhat, this is not an effective solution because the viscosity drops rapidly and the vapor pressure remains too high.

However, a very effective way to reduce the vapor pressure of the sorbent is to incorporate the amine functional group into an ionic liquid. Ionic liquids (ILs) are a relatively new class of compounds that can have low viscosity at room temperature and at the same time have effectively zero vapor pressure, even at molecular weights less than 100 g/mole [4]. A diagram of CO_2 control with a SLM is shown in Figure 1. The figure shows that CO_2 on the crew side of the membrane reacts with the sorbent, S, to form an intermediate complex. The intermediate then diffuses to the low pressure side of the membrane where the absence of gas phase CO_2 shifts the equilibrium state of the complex formation reaction. This causes the intermediate to decompose, releasing CO_2 to the low pressure side of the membrane and regenerating the sorbent.

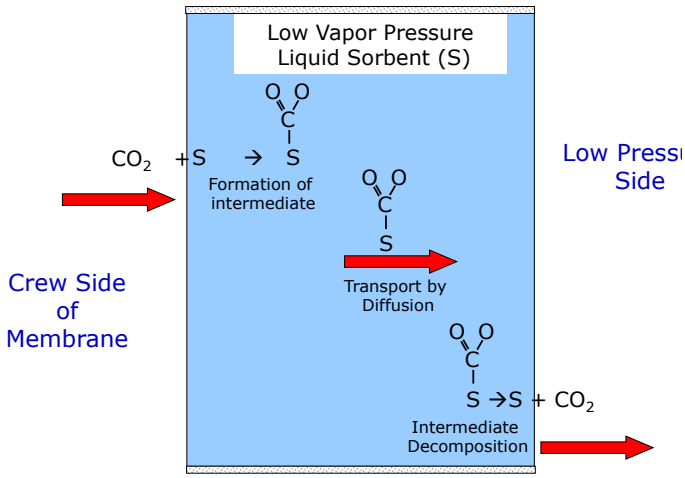

Figure 1. Schematic for facilitated CO2 transport within a membrane pore.

In a recently completed Phase II project, Reaction Systems developed an SLM for CO_2 control for application in the PLSS [5,6]. We fabricated a two layer, flat sheet SLM using an amine-functionalized ionic liquid, AP-Mim (Figure 2) as the sorbent. With this SLM, we obtained CO_2 permeance values up to 1.1E-4 scc/(cm^2 s cm Hg). We also measured an O_2 permeance of 7.6E-8 scc/(cm^2 s cm Hg), resulting in a CO_2/O_2 selectivity of 1450. These performance levels would be sufficient to permit the SLM to be used in the PLSS, if they could be achieved in a high surface area to volume form such as hollow fibers. Finally, in tests with representative humidity levels in the gas manifold, we found that the SLM has an H_2O permeance that is about 20 times greater than CO_2, and therefore the membrane can also be used to remove moisture. These results demonstrated the feasibility of using a supported liquid membrane for CO_2 control in the PLSS.

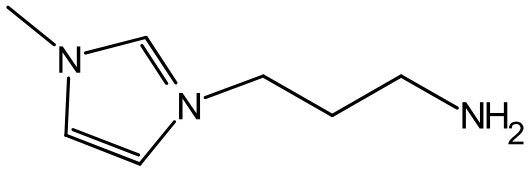

Figure 2. Structure of AP-Mim cation.

In order to use the SLM to control CO_2 in the cabin of a spacecraft and recover O_2, the low pressure side of the membrane would be connected to a vacuum pump instead of being exposed to space, as would be done in EVA. Cabin air is directed into the CO_2 SLM where CO_2 is removed from the main air flow. The vacuum pump reduces the total pressure on the low pressure side of the membrane, generating the driving force for CO_2 transport. The CO_2 rich mixture that penetrates the fiber walls to the low pressure side of the SLM is then pressurized to 0.9 atm so it can be directed into an oxygen recovery system such as a Sabatier reactor.

Although this is very promising technology, there are tasks that need to be carried to demonstrate the feasibility of using the SLM for cabin applications. First, the very promising performance obtained in the flat sheet needs to be transitioned into a more compact form to meet size requirements. The form with the highest surface area to volume ratio is a module containing a bundle of hollow fibers. In this configuration, the primary air flow goes through the inside of the fiber (lumen), while the outside of the fiber is maintained at low pressure and the ionic liquid sorbent is impregnated in the walls of the fiber. Therefore, one of the objectives of this project was to scale-up the module fabrication process so that a realistic assessment of this module configuration could be made. The second objective was to use the data obtained to date in order to produce a preliminary design of system to control CO_2 in the cabin to estimate the feasibility of this approach.

II. Experimental Methods

C. Compound Synthesis and Characterization

The sorbents used in this work consist of ionic liquids functionalized with an amine group. Ionic liquids are relatively low molecular weight hydrocarbon-based compounds that can have low viscosity and effectively zero vapor pressure. Thus, they are excellent choices for use in a SLM where one side will be exposed to space vacuum. In this work, we discuss results obtained with one containing a primary amine function group, 1-(3-aminopropyl)-3-methylimidazolium or AP-Mim. Once the sorbent was prepared, it was characterized by nuclear magnetic resonance (NMR) spectroscopy to verify its chemical structure. The methods used to synthesize and characterize this compound were described previously [5,6].

D. Fabrication of Hollow Fiber Modules

In order to meet the volume requirements for a CO_2 control system in the cabin and maximize the active surface area for CO_2 removal, the SLM membrane needs to be packaged in a form that has a high surface area to volume ratio. One such form is a hollow fiber module. Therefore, the first step in this project was to optimize the fabrication of hollow fiber supported liquid membrane modules. We fabricated two 1-in OD modules. In this case, we used a 1-in OD PVC pipe to house the fibers. Two ports were added to the side of the housing for urethane addition and connection to the vacuum source. These were made by drilling two holes in the side, tapping each with 1/8-NPT threads, and installing ¼-in Swagelok male connectors in each. Initial tests indicated that the pipe thread connections with or without Teflon tape did not provide an adequate seal. However, when threads of the connector were coated with epoxy cement, a leak tight seal was achieved.

Photographs of the 1-in OD module are shown in Figure 3 and Figure 4. The top photograph in Figure 3 shows the PVC housing and the fiber bundle outside of the module before it was potted into the housing. As shown, the fibers are long enough to extend out from each side of the module. The fibers were then inserted into housing, the red end caps attached to both ends of the module, and the ends of the module were filled with urethane from the two ports on the side as the module was rotated horizontally at about 300 rpm, enough to create about 9 G's of force. The caps retained the urethane and allowed it to fill the gaps between the fibers and the PVC wall creating an air tight seal. The bottom photograph shows the module after the potting process has been completed. The left side shows the section of the fibers potted in the urethane that extends outside of the PVC where the urethane was contained in the red cap. On the right side of the module, the photograph shows the module after the end of the bundle has been cut off at a point very close to the end of the PVC housing. Since the ends of the "as received" fibers are heat-sealed, this step is required to expose the inside of the fibers to the flow entering and exiting the module.

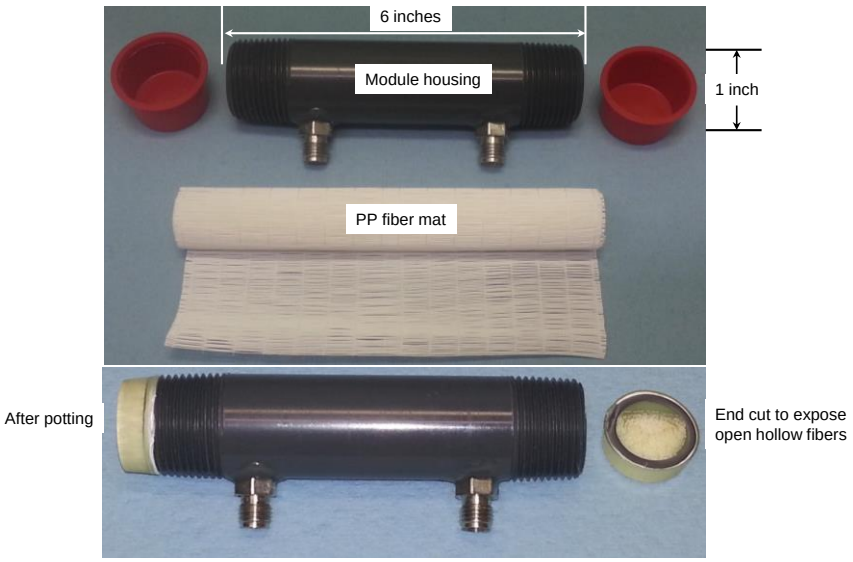

Figure 3. Photographs of the fabrication process of the 1-in module; top photograph: PVC housing and fiber matt before potting; bottom photograph: module after potting – left side before fiber ends have been cut off - right side after cutting the end off.

The top photograph in Figure 4 shows a close up of the end of the module after cutting to open the fibers. This module contains 1350 fibers, which results in an available surface area of 1120 cm^2. The bottom figure shows the module after the end caps have been added. Each cap has been fit with a threaded

Swagelok connector that will be used to connect the module to the main air flow. Prior to use, all of the threaded ports were sealed with epoxy to assure leak tight operation.

Figure 4. Photographs of the 1-in module; top photograph: end view showing open fiber ends; bottom photograph: module with end caps and threaded connectors.

Layered Structure

As pointed out in the introduction above, we were able to achieve the required performance in flat sheet form by using a two-layered membrane system. It consisted of a hydrophilic microporous membrane on the high pressure side and a hydrophobic microporous membrane on the low pressure side. The functionalized ionic liquid was contained within the hydrophilic membrane, and the presence of the hydrophobic membrane on the low pressure side prevented the liquid from being forced out the membrane by the pressure differential. Therefore, an analogous layered hollow fiber was needed to achieve comparable performance in the hollow fiber form.

Figure 5 illustrates the layered membrane in both the flat sheet and hollow fiber configurations. The left side shows the flat sheet layered membrane that produced the results described above. The right side shows a desired, analogous configuration in a hollow fiber form. In this configuration, the functionalized ionic liquid is contained within the pores of the wall of the hollow fiber, while a hydrophobic layer on the outside of the wall prevents the liquid from being forced out to the shell side of the membrane. The process flow is directed through the center of the hollow fiber (or lumen) while the shell side is exposed to vacuum. Thus, as the CO_2 contained in the air flows through the fiber, it is absorbed by the functionalized ionic liquid at the inside surface of the wall and then diffuses through the wall to the outside of the fiber where it desorbs into the vacuum.

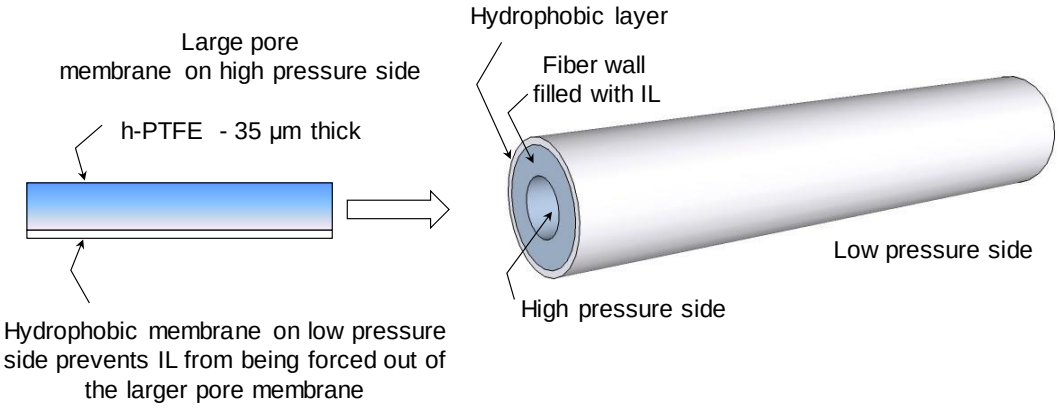

Figure 5. Two layer flat sheet membrane (left side) and the analogous two layer form in a hollow fiber (right side).

In this project, we used a uniformly microporous polypropylene (PP) membrane (Oxyphan from Membrana) that had a 380 µm OD, a 50 µm wall thickness, and a 280 µm ID. These hollow fibers were chosen because their OD was smaller than most other membranes available and they had the thinnest walls. The smaller OD allowed us to maximize the packing density and therefore the active surface area. The thinner HF walls, which were filled with IL, minimized the diffusion path through the membrane and maximized its rate of transport. Finally, the fibers have a uniform pore size and should be easier to fill with IL more evenly than we were able to do with previous fibers.

We also investigated several approaches to depositing a thin, dense, highly permeable layer on the outside of the PP HF. The coating on the outside of the fiber needs to have the right combination of CO_2 permeability and coating

thickness (P/L = Permeance) so that it does not slow down the transport of CO_2 across the SLM, and yet is durable and prevents the ionic liquid from escaping the pore walls. We identified a material that has very high gas permeability and can be coated on microporous PP hollow fibers at thickness of between 3 and 15 µm. The gas permeability of this material is high enough that these thicknesses should produce minimal resistance to mass transfer.

We prepared solutions of 1% and 3% polymer and coated the fibers by dipping the fiber mat into the solutions, quickly removing the fibers from the solutions, and then air drying the fibers in a fume hood to allow the solvent to evaporate to dryness. The coated fiber mats were then placed in a vacuum oven to remove any residual solvent.

E. Mixed Gas Test Rig

Gas permeation tests were conducted in a mixed gas test rig (Figure 6). The system circulates the process flow through the tube side of a shell-and-tube SLM module. Pressure transducers (PT-3 and PT-4) were fit to the loop in front of and downstream of the module to quantify the pressure drop through the device. The system includes an oil-less scroll pump to evacuate the loop, a gas manifold to charge the loop with representative pressures of N_2, O_2 and CO_2, a diaphragm pump to circulate the mixture, analytical instrumentation to measure the changes in CO_2 and H_2O concentrations, and an 8-liter reservoir. The mixture was circulated at a rate of about 10 slpm, resulting in a circulation time of about 30 seconds. An in-line, vacuum rated rotameter and valve controlled the flow in the loop. Water was introduce with a Chemyx Fusion 100 syringe pump so that water could be added on a continual basis at a representative rate. A Vaisala relative humidity sensor was used to monitor the relative humidity (RH) in the mixed gas. The sensor has a relative error of ± 1.5% RH over the entire range of operation. The CO_2 concentration in the gas mixture was monitored with a gas chromatograph (GC), equipped with a thermal conductivity detector (TCD). A silica gel column maintained at 100°C was used to separate CO_2 from either N_2 or O_2. Finally, the system used LabVIEW software and National Instruments hardware for control and data acquisition.

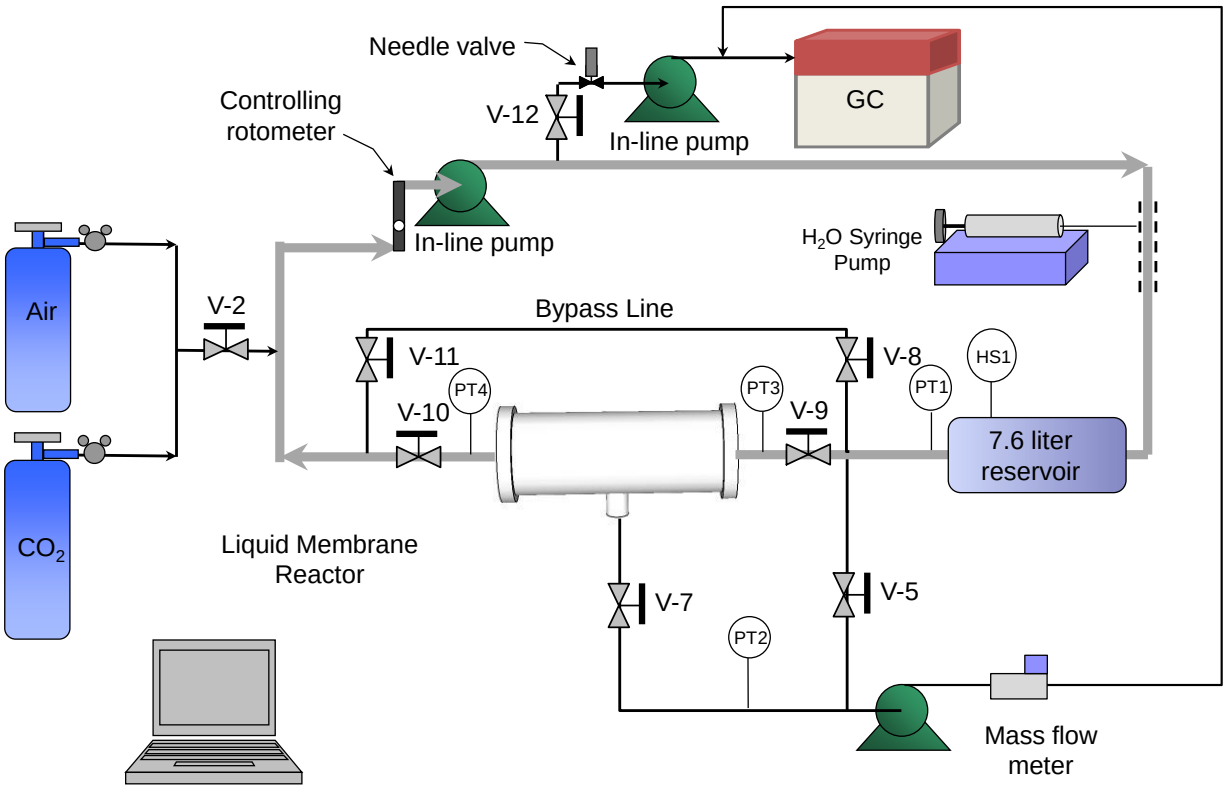

Figure 6. Schematic of the automated mixed gas test apparatus to measure CO_2 permeance in a cabin application.

To conduct gas permeation tests, the system was first evacuated to less than 50 mtorr by opening V-5 and V-7. We then closed V-5 and isolated the membrane by directing flow through the membrane bypass line. The loop and reservoir were then charged to 0.8 atm with a mixture consisting of 1% CO_2 in air (79:21 mix of N_2 and O_2), resulting in CO_2 partial pressure of 6 mmHg. The circulation pump was started and the temperature of the module was then

raised to the desired set point and for tests using continuous water addition, the syringe pump was activated and water was injected at a rate of 8.0 µL/h to bring the humidity level up to the desired set point. Baseline GC measurements were obtained to verify that the expected CO_2 concentration was achieved in the loop and then the process flow was switched from the membrane bypass loop to the flow-through cell, exposing the process flow to the SLM. During the entire test, V-7 remained opened, reducing the downstream CO_2 partial pressure to less than 50 mtorr. Measurements of CO_2 concentration in the loop were made through the course of the experiment.

CO_2 permeance was calculated by converting the change in concentration to mass flow through the membrane normalized by the pressure differential. To measure air permeance, the syringe pump and the pump to the GC were stopped and then the change in total pressure was monitored, converted to mass flow, and converted to permeance using the total pressure in the system.

III. Results

F. Mixed Gas Test Results with Polymer-Coated Fibers in the 1-in OD Module

An example of typical data obtained during a test with the 1-in modules is shown in Figure 7. This module was impregnated with a recently prepared ionic liquid and contained a total quantity of 6.64 grams of this sorbent. The square data points represent a single GC analysis while the solid line is the total pressure in the manifold. At the beginning of test, the CO_2 concentration was 0.95 mole%, which is equal to a partial pressure of 6.1 mm Hg. When the manifold was opened to the module the CO_2 concentration dropped rapidly and reached a value of 0.1 mole% in a period of 270 min or 4.5 hours. Since this is a batch process, we calculate permeance by measuring the slope of the line and then normalize it with the CO_2 partial pressure at that point. As shown, we obtained values of 1.45 E-5 scc/(cm^2 s cm Hg) after two hours in the first exposure and obtained a similar value after we recharged the manifold.

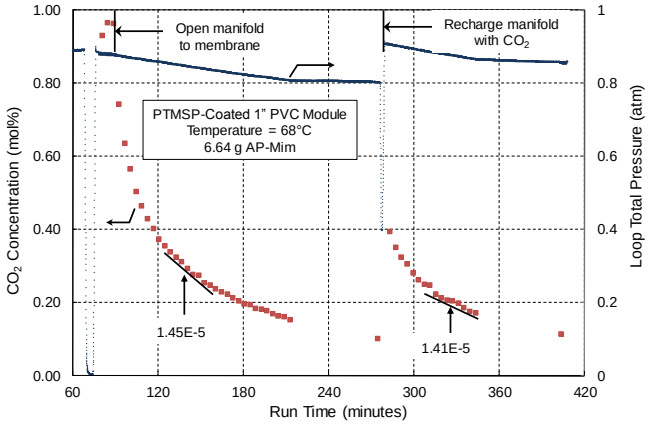

Figure 7. CO_2 concentration during a test with a 1-in module. Arrows mark points where the permeance was calculated.

Summaries of the results obtained for this module are shown in Figure 8 and Figure 9. Figure 8 shows the CO_2 and air permeances while Figure 9 presents the CO_2/air selectivities over the temperature range. The CO_2 permeances ranged from 1.22E-5 scc/(cm^2 s cm Hg) at an exit temperature of 60.8°C up to 1.55E-5 scc/(cm^2 s cm Hg) at 78°C. The selectivities for CO_2 over air for this module are shown in Figure 9. We obtained values ranging from 217 at 60.8°C to 112 at 78.1°C. At this selectivity, the concentration of CO_2 exiting the module through the permeate will be relatively high, which will reduce the power required for the pump on the low pressure side of the module. However, the O_2 and N_2 concentrations would exceed the target of 1 vol% and 2 vol% for entering the Sabatier.

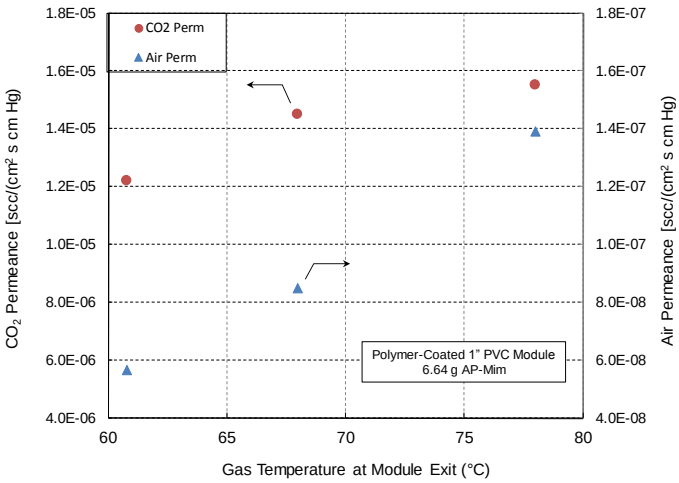

Figure 8. CO_2 and air permeance results obtained with the 1-in diameter module containing polymer coated polypropylene fibers and 6.64 grams of fresh IL.

We also carried out tests on a second module containing 10.14 g of a batch of AP-Mim that had been synthesized several months earlier. Overall the CO_2 and air permeances were lower than those obtained in the previous test while the CO_2/air selectivities were similar. One potential cause of the lower permeances is a higher loading of IL. The latter module contained 10.14 grams of IL, while the previous module contained 6.64 g IL. The higher IL loading would reduce the flow rate of both CO_2 and air, which is consistent with the results obtained.

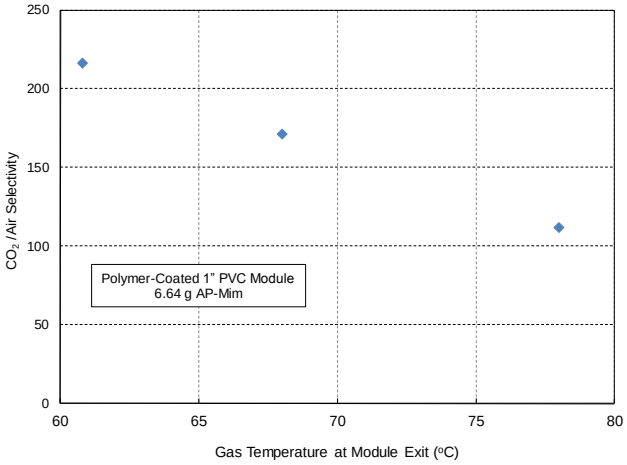

Figure 9. CO_2/ air selectivity values obtained with 1-in diameter module containing polymer coated polypropylene fibers and 6.64 grams of fresh IL..

Overall the similarity in performance obtained by the two 1-inch modules leads to two conclusions. One conclusion is that it is likely that all of the pore volume contained ionic liquid sorbent and the use of the more uniform pores resulted in a more consistent impregnation process, which was required in order to evaluate the feasibility of using hollow fiber modules. The second conclusion is that the limitations in types of hollow fiber materials that are available make it unlikely that the CO_2 permeance and selectivity we achieved in the flat sheet membrane can be achieve in the hollow fiber form. Thus, it is necessary to evaluate other compact module configurations. This will be discussed in more detail in Section H.

G. H_2O Permeance Tests

In an SLM system it may be necessary to remove the moisture from the flow prior to directing it into the main CO_2 module and before it is heated. Although we had seen that moisture permeated through the membrane rapidly and had estimated the permeance at elevated temperature, we had not carried out a test at ambient temperature. We therefore conducted a test to measure the moisture permeance of the SLM at ambient temperature. We used the 1-in module that contained 6.64 grams of the more recently prepared ionic liquid. To conduct the test, we injected H_2O into the manifold at various rates and at each rate measured the steady state RH that resulted. At that point, the flux through the membrane can be calculated from the injection rate. The exposure pressure is equal to the differential pressure across the membrane and in these tests with the high flow of water, we observed that the water partial pressure in the volume downstream of the module rose and therefore we subtracted this pressure from the pressure in the circulation loop.

The results of this test are shown in Figure 10, which shows RH in the circulation loop during the test. Before the manifold was opened to the module, we began injecting water at a rate of 150 µL/min and the RH rose rapidly. However when we opened the module to the manifold the RH dropped quickly to 5% and then averaged about 7% at that injection rate. At 250 minutes, we increased the injection rate to 250 µL/min and the RH stabilized at about 9%, which is equivalent to a pressure of 2.73 mm Hg. The pressure downstream of the module was 0.53 mm Hg resulting in a net pressure differential of 2.2 mm Hg. With these values we obtained a water permeance of 5.86E-4 scc/(cm^2 s cm Hg) at 25°C.

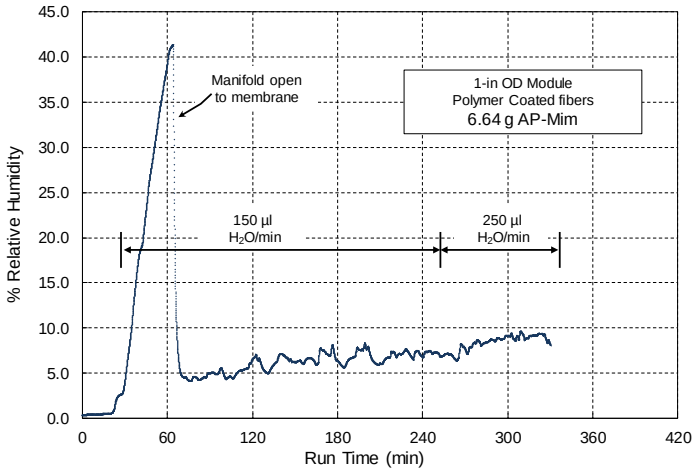

Figure 10. RH measurements at different H_2O injection rates with a 1-in diameter module containing polymer coated polypropylene fibers.

H. Conceptual Design of a Full Scale SLM System

We used the data obtained in this project along with our Phase II project to carry out a conceptual design of a system that would use a supported liquid membrane for CO_2 control and maintain the cabin level at 2 mm Hg. In all calculations of pump or heater power, we initially calculated the power required without including inefficiencies or energy losses. We then applied appropriate efficiency estimates or heat losses to obtain more representative power and size estimates. Sources for the specific efficiencies used are cited in the discussion of each component.

System Overview

A schematic of the components anticipated in the design are shown in Figure 11. The figure includes text showing the conditions at the inlet of the system and then shows the parameters in the flow that undergo the most significant change through each unit. We also included position numbers, which identify positions in the process for future reference. In this section we present a general description of the components and their function. In the following section we include more details on the performance of each component.

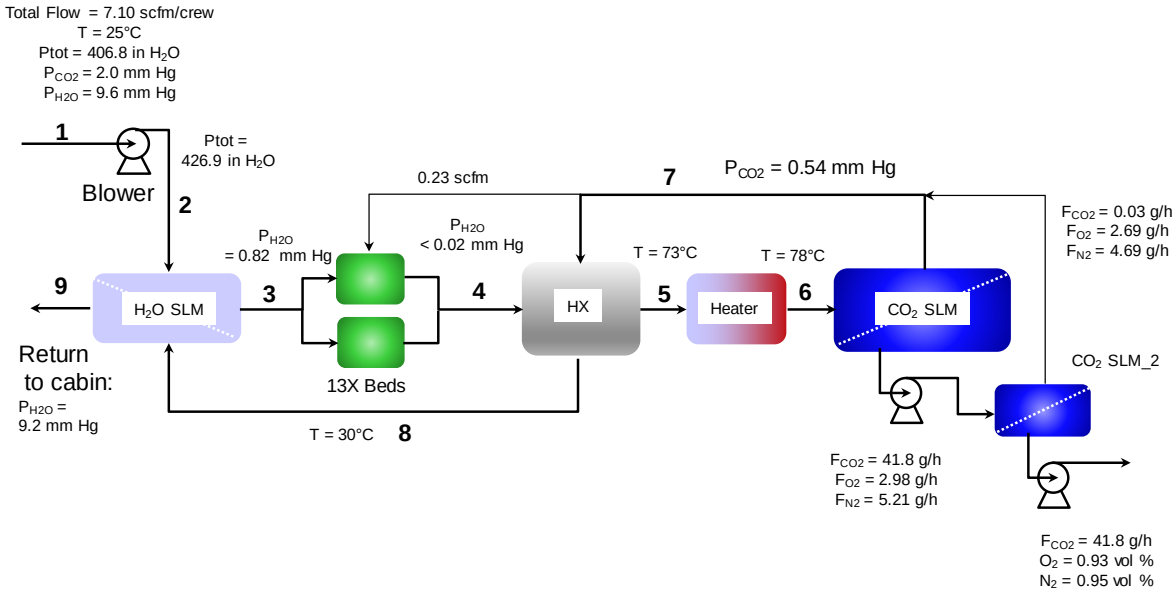

Figure 11. Schematic of the SLM CO_2 removal system.

The system consists of a blower that moves the air flow through all components. The total flow rate is set by the CO_2 generation rate, the maximum allowable concentration in the cabin, and the module efficiency. The CO_2 generation rate was assumed to be 1 kg CO_2 per crew per day and the maximum allowable CO_2 concentration was set to 2 mm Hg. As we will discuss, the module efficiency is 74% so the required flow into the system is 7.1 scfm per crew resulting in a total pressure drop of through all components will on the order of 25 inches of water. As shown in the figure the moisture content in the flow is 9.6 mm Hg, or RH = 40%. The air first enters an H_2O SLM module for moisture removal. This SLM transfers a high percentage of the moisture from the incoming air to the dry, processed air that is being returned to the cabin.

Although our data suggest that water vapor does not have a measurable effect on the performance of the SLM for CO_2 control, water permeates rapidly through the CO_2 SLM. Therefore, most of the moisture in the flow would permeate the main CO_2 membrane along with the CO_2 flow, and the air returning to the cabin would be too dry. The H_2O SLM will operate at ambient temperature and will contain a non-functionalized ionic liquid so it will not remove CO_2 from the flow. However, because, water is very soluble in ionic liquids, the moisture will permeate rapidly through the membrane. The flow is then directed through one of two small Zeolite 13X beds that removes the remaining moisture in the flow. We used the Toth equation from Wang and Levan (2009) to estimate the time for the bed to become saturated based on the moisture flow into the bed. These beds will operate in a similar fashion as is done currently in the CDRA. One bed will be in the adsorption mode while the other is being regenerated with a small

flow that is split off from the hot dry air exiting the CO_2 removal SLM. The flow then enters a recuperative heat exchanger, with a designated effectiveness of 0.90. The temperature of the air returning from the module, or entering the hot side of the heat exchanger, is set to 78°C, which is the temperature where we obtained the best performance with our SLM. With the specified efficiency and hot side temperature, the temperature of the air exiting the heat exchanger on the way to the CO_2 module can be determined and we obtained a value of 73°C. The air then is directed through a heater where the temperature is raised from 73°C to 78°C prior to being directed into the main CO_2 SLM where CO_2 is removed from the main air flow. The main air flow leaving the module then passes back through the heat exchanger where the temperature is dropped to 30°C and then through the first SLM where it is re-humidified and returned to the cabin. A compressor is used to maintain a low pressure on the permeate side of the CO_2 module. However even with very high selectivity, the concentrated CO_2 in the permeate flow contains higher concentrations of N_2 and O_2 than are allowed to be fed into the Sabatier. Consequently, the permeate flow is directed through a second SLM, which reduces the N_2 and O_2 concentrations to less than 1%. Since the CO_2 concentration entering this membrane is very high, the module can be small and the power requirement for the pump on the low pressure side is very low. The performance of each of these component is discussed in more detail in the following sections. A summary of volumes and powers is included at the end of this section.

Main CO_2 Removal Module

In the work we have carried out in this project and in our previous Phase II SBIR project, we tested our SLM in the flat sheet and hollow fiber configurations [5]. The drawing on the left side of Figure 5 shows the SLM in a flat sheet form while the drawing on the right side shows a SLM in the hollow fiber format. The hollow fiber configuration is desirable because of its high surface area to volume ratio. For example, a hollow fiber module can have surface area to volume ratios of up to 200 m^2/ft^3 and the hollow fiber modules we prepared, in which the bundles were not packed as tightly as possible, had measured values of about 97 m^2/ft^3. On the other hand, stacked flat sheet modules generally have surface to volume ratios that are much lower.

However as shown above, we were not able to achieve the performance in the hollow fiber modules that we did in the flat sheet configuration and therefore we identified other module configurations that could be used. For example, reasonably high surface to volume ratios, up to 50 m^2/ft^3, can be achieved when a flat sheet is wrapped into a spiral wound configuration (see Figure 12). As shown in the figure, in a spiral wound module, a polymer membrane is wrapped around a permeate manifold and the process flow is directed though the end of the wrapped layers from one side to the other. The membrane layers are separated from each other with mesh spacers and in an SLM application, all membranes layers are impregnated with ionic liquid. This is a very common configuration and has a good combination of surface to volume ratio and low pressure drop. Moreover, using this configuration will allow us to utilize the wide variety of membrane materials that are commercially available and still provide good access to the membrane surface so pores of the membrane can be filled efficiently with the functionalized ionic liquid.

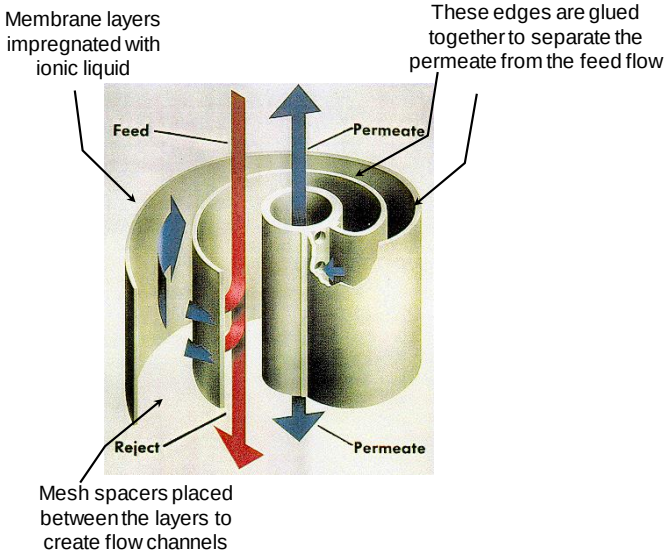

Figure 12. Schematic spiral wound membrane (from [7]).

Therefore, we completed the conceptual design of a CO_2 control module using performance data we obtained in the flat sheet configuration and applied a surface to volume ratio typical of a spiral wound module. In tests carried out in Phase II, we achieved a CO_2 permeance of 1.1E-4 scc/(cm^2 s cm Hg) and a CO_2/O_2 oxygen selectivity of 1410 at a temperature of 78°C using the ionic liquid we developed for this purpose, AP-Mim [5,6]). We therefore used these values to estimate the required module size assuming a surface to volume ratio of 50 m^2/ft^3. We also used these results to estimate the power required for the pump on the low pressure size of the module and the composition of the gas in the permeate. As pointed out above the design was based on a CO_2 generation rate of 1 kg/day or 41.8 g/h and a maximum

CO_2 partial pressure at 2 mm Hg. In our modeling approach, which is described below, we calculated the needed membrane surface area to obtain the required performance and then used the surface area to volume ratio for spiral wound modules (50 m^2/ft^3) to calculate the module size.

We developed a numerical integration model to estimate the module performance. The model divides the module into small segments and uses the flow conditions to calculate the residence time in each segment. It then uses the permeance, partial pressure difference, and surface area in the increment to calculate the amount of CO_2 that would permeate out of the process flow in the residence time and then updates the concentration that would be contained in the next segment. The model allows us to calculate performance as a function of a number of variables including length and diameter of the modules along with flow rate at the specified incoming CO_2 partial pressure of 2 mm Hg. For a given size, higher feed flow rates will result in lower percent CO_2 reductions and higher pressure drop while lower flow rates produce higher percent CO_2 reductions and lower pressure drops. However, at higher flow rates, the partial pressure of CO_2 remains higher in the module producing a greater driving force and therefore a higher overall rate per unit membrane area.

The model prediction of CO_2 partial pressure as a function of module length is shown in Figure 13. In our design we selected a module size that contain a membrane surface area of 53.7 m^2. With these conditions and a flow of 7.1 scfm, we obtained a CO_2 partial pressure at the module exit of 0.54 mm Hg resulting in the required removal rate of 41.8 g/h. In the hollow fiber configuration this area could be contained in a volume of 0.56 ft^3 and in a spiral wound configuration, it would occupy a volume of 1.07 ft^3.

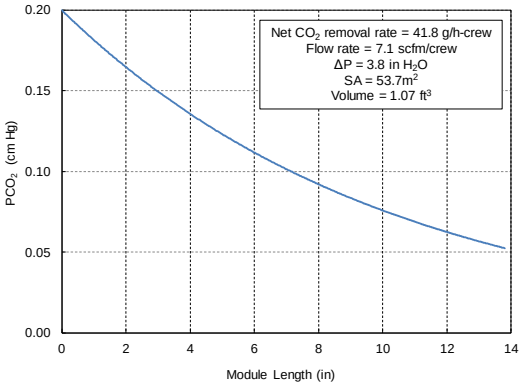

Figure 13. CO_2 partial pressure as a function of length through the module.

We also calculated the pressure drop through the membrane module. In this case we assumed a hollow fiber configuration, and since hollow fibers have higher pressure drops for similar surface area compared to spiral wound modules, this represents a worst case condition. We used the Darcy–Weisbach equation to calculate the pressure drop:

$$\Delta p = fd * L/D * \rho V^2/2 \quad (1)$$

where fd is the Darcy friction factor, defined as 64/Re, Re is the Reynolds Number = $\rho Vd/\mu$, L/D is the length to diameter ratio of the hollow fibers, ρ is the fluid density and V is the fluid velocity through the fibers. We used the physical dimensions of the polypropylene hollow fibers that were used in the 1-in module fiber for the calculation. These fibers have an inner diameter of 280 µm and the module contained 379 fibers per cm^2. With this relationship, we obtained a pressure drop of 3.6 in H_2O through a module that has an surface area 53.7 m^2.

We also verified the pressure drop calculation by measuring the pressure drop that occurred through the 1-in module as a function of flow rate. Figure 14 compares measured data in the 1-in diameter module versus calculated values. The figure shows that although the measured values are somewhat higher than the predicted values, the differences are within 15%. Therefore, in our design, we adjusted the pressure drop calculation by adding 15% to the calculated value.

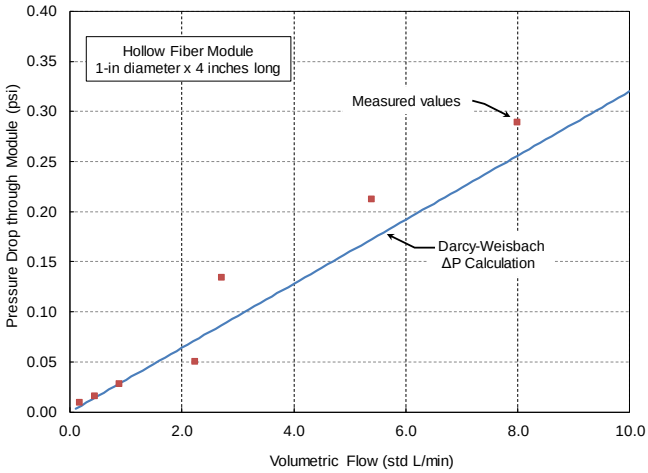

Figure 14. Pressure drop measured vs calculated values.

Main Compressor Power

As shown in Figure 11, a vacuum pump is used to decrease the pressure on the permeate side of the membrane. The power required for this pump depends on pressure difference across the pump and total flow. The flow through the permeate side of the CO_2 SLM consists of 41.8 g/h CO_2, 5.21 g/h N_2 and 2.98 g/h O_2. We assumed that the pressure on the permeate side of the membrane was 50 mtorr and that the permeate flow on the high pressure side of the pump was 1 atm. We calculated the required compressor power using the equation shown below:

$$P = m\,\gamma/(\gamma\text{-}1)\,R\,T\,[(P_2/P_1)^{(\gamma-1)/\gamma} - 1] \qquad \text{Eq. 2}$$

Where P is power in kW, m is the mass flow, γ is the isentropic expansion factor for CO_2, R is the gas constant, T is absolute temperature, P_2 is the pressure at the compressor outlet and P_1 is the pressure on the low pressure side of the compressor [8]. Using the flow rates listed above, we obtained a required compressor power of 26.8 watts.

Permeate Flow Processing

As described above, the flow to the Sabatier reactor requires a CO_2 flow that is dry and contains less than 1%O_2 and 2% N_2 by volume. However, the mass flows listed above are equivalent to volumetric flows of 7.5% O_2 and 15.1% N_2. Therefore, this flow must be purified before it can be delivered to the Sabatier reactor.

One way to purify this flow is direct it through a second SLM. In this case, the concentration of CO_2 is very high while the concentrations of N_2 and O_2 are lower compared to the cabin air. Therefore, the size of the module can be much smaller and the pressure on the low side can be higher than 50 mtorr, which will reduce the compressor power. We modified our SLM model to simulate the second stage SLM. In this case, we set the module surface area to 1.2 m^2 which would occupy a volume of 0.02 ft^3 in a spiral wound configuration. The partial pressures of CO_2, N_2, and O_2 in the process flow are shown in Figure 15 as a function of length through the module. The model predicts rapid loss of CO_2 and increasing partial pressures of N_2 and O_2 at the end of the module.

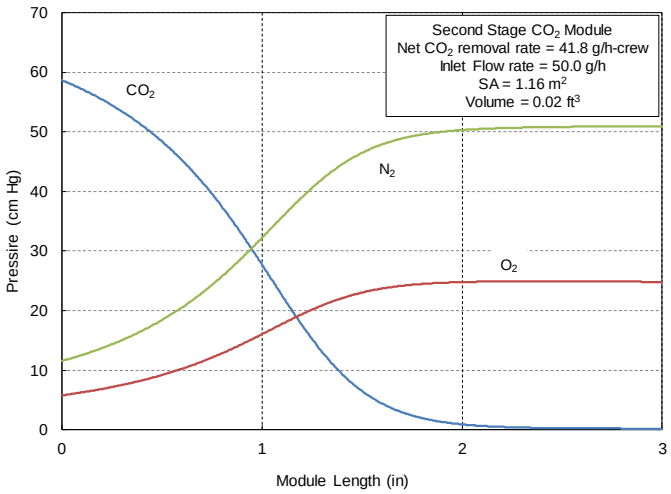

Figure 15. Partial pressures of CO_2, N_2, and O_2 as a function of length through the second stage SLM.

A process schematic of the two stage system is shown in Figure 16. The flow going to the Sabatier reactor contains almost all of the CO_2 coming into the second stage of the SLM and is very pure, containing only 0.50 volume % O_2 and 0.51 volume % N_2. Finally, only 0.03 g/h CO_2 is being returned to the cabin. This flow is equivalent to a partial pressure of less 0.01 mm Hg and therefore is not high enough to change the partial pressure of 0.54 mm Hg that was exiting the first stage of the CO_2 membrane. Finally the figure shows that this performance was attained with a lower differential pressure across the second stage compressor, which reduces the overall power demand. We used a pressure of 2000 mtorr on the low pressure side of the second stage module and allowed the compressor to raise the pressure 0.9 atm for direct introduction into the Sabatier reactor. With the reduced pressure differential and the reduced flows of N_2 and O_2 going through the second stage compressor, the required power for the second stage compressor is 7.5 watts.

SLM for Moisture Removal

Although water vapor does not have a measurable effect on the performance of the SLM for CO_2 control, it will permeate rapidly through the CO_2 SLM, which would cause the cabin air to be too dry. The H_2O SLM will take most of the moisture out of the incoming air and return it to the processed air as it is returned to the cabin. This module will operate at ambient temperature and will contain a non-functionalized ionic liquid so it will not remove CO_2 from the flow. As described earlier, we carried out a separate test in a 1-in module with AP-Mim to measure the H_2O permeance

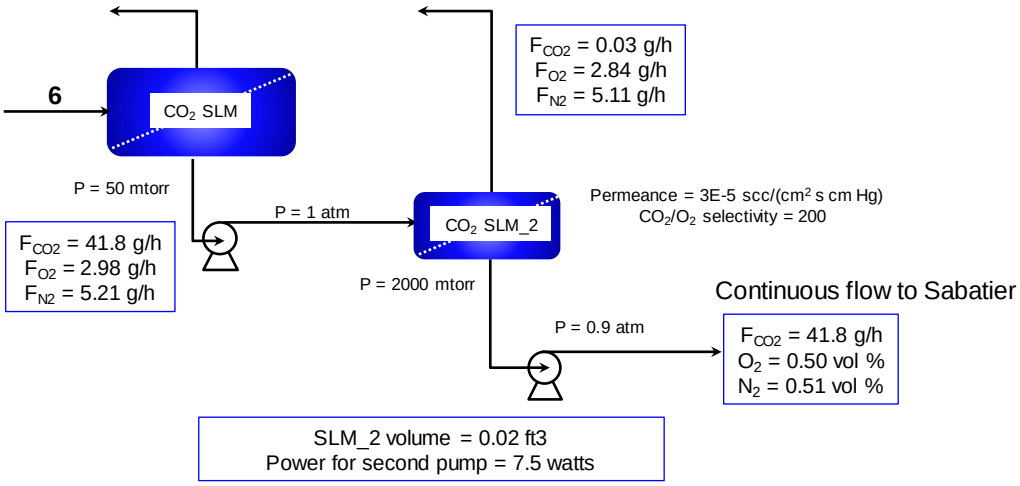

Figure 16. Diagram of a two stage SLM and the flows of CO_2, N_2, and O_2 going back to the cabin and into the Sabatier reactor.

at room temperature and obtained an H_2O permeance of 5.86E-4 scc/(cm^2 s cm Hg). To size this module, we used the numerical model developed to evaluate CO_2 performance and set the permeance to the value listed above. Instead of using a pump to reduce the vapor pressure on the low pressure side, this module utilizes the dry flow exiting the CO_2 SLM module in a counter current flow. We set the H_2O concentration entering the sweep side of the module to zero and the concentration exiting the module on the sweep side to approximately 8.8 mm Hg and assumed a linear profile going through the module. We then used the H_2O permeance and the difference between the H_2O pressure entering the main flow path to the sweep pressure and calculated the concentration exiting the module in the main flow path. Figure 17 shows that the partial pressure on the process side is 0.082 cm Hg or 0.82 mm Hg.

There is a trade-off here between the size of this module and the size of the 13 X beds located downstream of this SLM and the power required to regenerate the beds. We found that a good balance between module size and power for regeneration was obtained if the SLM was sized to reduce the H_2O pressure to 0.82 mm Hg. Using this approach, we found that a membrane surface area of 79 m^2 was needed. Moreover, since the H_2O permeance data was obtained in a hollow fiber module, we used a hollow fiber surface area to volume ratio to determine that the required surface area could be contained in a volume of 0.84 ft^3.

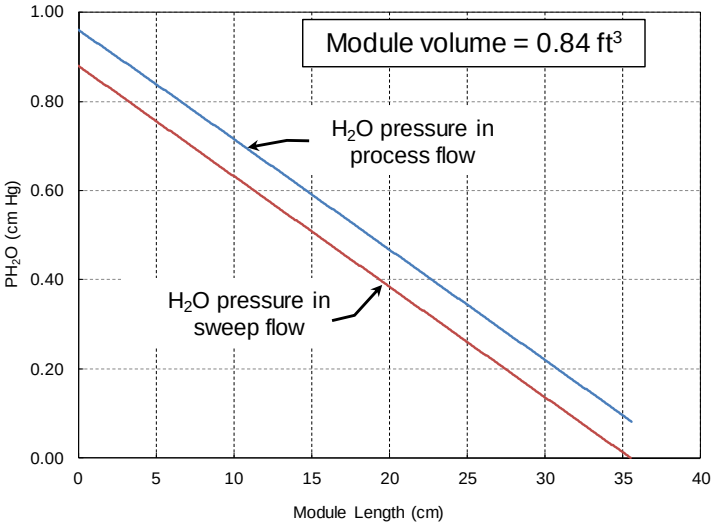

Figure 17. Partial pressures of water in the process flow and in the sweep gas in a SLM for moisture control.

H_2O Sorbent Bed

The flow exiting the H_2O SLM is then directed into one of two beds packed with zeolite 13X that will reduce the water concentration to less than 0.002% RH (DP <-47°C). Reducing the concentration of water to this level would prevent condensation if the concentrated CO_2 flow is compressed prior to being fed into the Sabatier reactor. However, higher water levels may be tolerated if the flow exiting the system is fed directly into the Sabatier and does not require compression. During operation, one bed is used to adsorb moisture, while the other is being regenerated by heating with a flow of dry air, similar to the strategy currently employed on the CDRA. However, in this case, the zeolite beds are required to remove only a small fraction of the ambient air humidity and can therefore be much smaller than the beds on the CDRA and also be regenerated less frequently.

As shown in the figure, the partial pressure of water entering the beds is 0.82 mm Hg (RH = 3%), less than one tenth of the ambient air moisture concentration. We used the Toth equation from Wang and Levan[9] to estimate the bed capacity and the time for the bed to become saturated based on the moisture flow into the bed. At 0.82 mm Hg moisture flow and using the constants for 13X from Wang and Levan, we obtained a total capacity of 20.1 wt%. However, before the bed reaches capacity, breakthrough would begin and to avoid allowing any moisture through the bed we set the capacity at 60% of the full value or 12.1 wt%. With that capacity, each bed can stay on line for 8.7 hours before it requires regeneration. Specific regeneration conditions are to be determined, but since the bed is relatively small not much power would be required. One strategy would be to split off a small flow of dry warm air from the exit of the main CO_2 module to use as a sweep gas for regeneration. Heating each bed from ambient temperature to 150°C every 8.7 hours requires an average power of 2.1 watts. The average air flow needed to contain the moisture in each bed is 0.23 scfm. Heating this air flow from 78°C to 150°C requires an average power of 10.2 watts, resulting in a total average power for the zeolite 13X beds of 12.3 watts.

The pressure drop through the bed was calculated using the Ergun equation assuming particle size of 0.1 cm, a void fraction of 0.45 and a bed that was 4 inches in diameter by 5.25 inches in length resulting in a volume of 0.05 ft^3 per bed. Using these parameters, we obtained a pressure drop of 12.1 inches of H_2O.

Heat Exchanger

The dry flow exiting the 13X bed is directed into a recuperative heat exchanger that uses the energy from the hot flow exiting the module to warm the flow entering the module. The four temperatures of the two flows going through the heat exchanger are shown in Figure 18. The stream leaving the 13X bed is called the cold side and the flow leaving the CO_2 control module is referred to as the hot side. Thus, we have cold side temperatures in and out (T_C in and T_C out respectively) and hot side temperatures in and out (T_H in and T_H out) respectively. Effectiveness is defined in terms of these temperatures as shown below

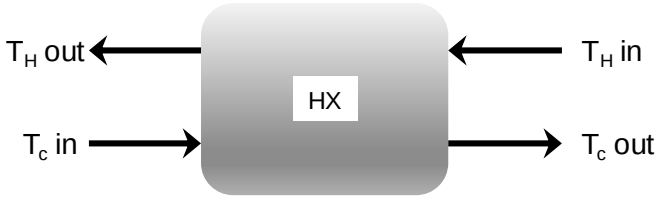

Figure 18. Flows entering and exiting the recuperative heat exchanger.

$$E = (T_C \text{ out} - T_C \text{ in})/(T_H \text{ in} - T_C \text{ in}) \quad (3)$$

Therefore, the temperature exiting the heat exchanger going to the heater (T_C out) is given by:

$$T_C \text{ out} = E * (T_H \text{ in} - T_C \text{ in}) + T_C \text{ in} \quad (4)$$

If we assume that the module will operate at a temperature of 78°C and the heat exchanger effectiveness is 0.90, then

$$T_C \text{ out} = 0.90 * (78°C - 25°C) + 25°C = 73°C \quad (5)$$

If we assume that the specific heats of the flows on each flow are equal, the temperature of the hot flow exiting the module (T_H out) would decrease by the same amount that the cold side temperature increased. The cold side temperature increased by 45°C and therefore the hot side temperature will decrease by 45°C and leave the heat exchanger at a temperature of 30°C, only 5°C warmer than the incoming air flow.

A plate and fin design was used to size the heat exchanger. The unit consisted of alternating flow paths with cells that are 1 cm high by 0.1 cm in width with width of 5 cm that resulted in 50 flow channels. The hot and cold side heat transfer coefficients are:

$$h = 0.085 \, Re^{-0.265} \, Pr^{-2/3} \, Cp \, G \quad (6)$$

where Re is the Reynolds number, Pr is the Prandtl number, Cp is heat capacity of air and G is the mass flux. We obtained a Reynolds number of 720 and a mass flux of 8.67 kg/(m^2 s) respectively on the cold side and 700 and 8.43 kg/(m^2 s) respectively on the hot side. The Prandtl number and heat capacity for air are reported to be 0.709 and 1.01E

3 J/kg K (Engineer's Tool Box, 2015). Thus, we obtained heat transfer coefficients of 126 W/(m^2 s) on the cold side and 123 W/(m^2 s) on the hot side. Therefore, the overall heat transfer coefficient (U), which is given by:

$$1/U = 1/h_c + 1/h_h \quad (7)$$

is equal to 62 W/(m^2 s).

If the mass flow and heat capacities of each flow are equal then the total surface area required for the heat exchanger is given by:

$$A = m\ C_p\ NTU/U \quad (8)$$

where NTU = E/(1-E), and m is the mass flow. Using the values listed above, we obtained an area of 0.39 m^2. The surface area to wetted perimeter of the heat exchanger described above is 0.045 cm^2/cm. With a front area of 5 cm^2, the area to length ratio of the heat exchanger is 110 cm^2/cm or 1.1 m^2/m. Thus the required length of this heat exchanger is 0.36 m or 36 cm. This results in an overall volume of 0.0058 ft^3.

Finally, the pressure drop through the heat exchanger was calculated using the following equation below:

$$\Delta p/\Delta L = 7.04\ Re^{-0.547}/\rho\ De \quad (9)$$

Where ρ is the fluid density and De is the effective channel diameter (4* Ac/Aw) where Ac is the area of the channel and Aw is the wetted perimeter. The calculated pressure drop through this unit is < 0.1 inches H_2O/meter and therefore the total pressure drop is < 0.01 inches of H_2O.

Heater for CO_2 SLM

The final component prior to reaching the CO_2 module is the heater to raise the temperature from 73°C to 78°C. With the flow and temperature rise we calculate a total power requirement of 21.4 watts. This is a relatively low power requirement and could be achieved by wrapping heat tape around process lines. Thus, there is no additional pressure drop or increase in volume.

Blower

Since there is very little pressure change in the overall air flow through the system, we used a relation for incompressible flow to calculate the blower power and this is simply the product of the volumetric flow and pressure change as shown below:

$$Power = Q * \Delta p \quad (10)$$

where Q is the volumetric flow rate and Δp is the pressure differential [10]. Fortunately, in this system, there is only one packed bed for the flow to pass through and the pressure drops for the liquid membrane modules are relatively low. As shown in the Figure 11, the blower only needs to raise the pressure from 406.8-in H_2O to 426.9 in H_2O or by 20.1 in H_2O. With this pressure drop and the total flow of 7.1 scfm or 200 slpm, we obtain a power of 17.2 watts.

1.1.1 Design Summary

Table 2 lists the temperatures, pressures, CO_2 pressures, and H_2O concentrations at the locations shown in the system schematic that was presented in Figure 11. As shown, the flow of 7.1 scfm enters the system (Position 1) with a CO_2 partial pressure of 2 mm Hg, a RH of 40% and at a total pressure of 406.8 in H_2O (1 atm). The blower raises the pressure to 426.9-in H_2O (Position 2) and then the flow enters the SLM module for moisture removal where the H_2O partial pressure is decreased to 0.82-in H_2O. The flow then passes through one of 13X beds where the remaining water is removed as shown at Position 4 and then is directed through the recuperative heat exchanger and then over a heater where the temperature of the flow is raised to 78°C (Position 6), which is the temperature where we obtained the best membrane performance in the SLM. The SLM reduces the CO_2 concentration to 0.54 mm Hg (Position 7) and then the flow passes through the heat exchanger where the temperature is reduced to 30°C (Position 8). As shown

Table 2. Flows, temperatures, CO_2 pressures and H_2O concentrations as a function of location in the SLM system.

Position	1	2	3	4	5	6	7	8	9
Flow rate (scfm)	7.1	7.1	7.0	7.0	7.0	7.0	7.0	6.8	6.8
Temperature (°C)	25	25	25	25	73	78	78	30	27
PTOT (in-H2O)	406.8	426.9	424.4	412.3	412.2	412.2	408.1	408.0	406.8
PCO2 (mm Hg)	2	2.1	2.1	2.1	2.1	2.1	0.54	0.54	0.53
PH2O (mm Hg)	9.6	10.1	0.82	<0.02	<0.02	<0.02	<0.02	<0.02	9.2
RH (%)	40	42	3	<0.1	<0.1	<0.1	<0.1	<0.1	39
DP (°C)	8.6	9.1	-17.7	<-52	<-52	<-52	<-52	<-52	8.1

in the figure, a small portion of the warm dry flow is split off from this flow and used as a sweep gas during the 13X bed regeneration. An average flow of 0.23 scfm would be needed to contain the moisture collected on each bed. Since it is already warm and dry, utilizing this flow reduces the power required to warm the regeneration air. Finally, the balance of the flow is directed through the sweep side of the H_2O removal module where the flow is humidified to a H_2O concentration of 9.2 mm Hg (RH = 39%) and returned to the cabin.

A summary of the power requirements for the components in the system are listed in Table 3. We have included the base level power without any losses or inefficiencies. We also have included a column that accounts for these unavoidable factors. We used data provided by NASA from the CDRA operation. Based on power consumed, mass flow, and pressure differentials provided, we calculated that the efficiencies of the compressor and blower are 26% and 46% respectively. Heat losses are 30% of the power input. As shown the highest component power is for the compressor on the main CO_2 module which requires a power of 26 watts. The powers for the heater and blower are 21.4 watts and 17.2 watts. The overall base power required is 84.2 watts, well below the value of 118 watts as outlined earlier. The total power with compressor and blower efficiencies and heat losses factored in are 213.7 watts.

Table 3. List of power requirements.

	Min Power	CDRA Effic
Unit	watts	watts
Blower (46%)	17.2	37.3
13X Bed heater (30% losses	11.4	16.4
SLM Heater (30% losses)	21.4	30.6
CO2 SLM Pump (26%)	26.8	101.4
CO2 2nd Stage (26%)	7.4	28.1
Total	84.2	213.7

Table 4 lists the size estimates of the main components in the system. The largest units are the CO_2 and H_2O SLM, which occupy volumes of 1.07 and 0.84 ft^3 respectively. As shown, the total volume in this design is 2.04 ft^3.

Table 4. Size estimates of the SLM system components.

	Size
Unit	ft3
H2O SLM	0.84
13X Bed	0.10
HX	0.01
CO2 SLM	1.07
CO2 2nd Stage	0.02
Total	2.04

IV. Conclusions

This paper demonstrates the feasibility of using an SLM system to control CO_2 at a maximum concentration of 2 mm Hg. We identified a module configuration that has a high surface area to volume ratio and, using membrane performance data that we measured in a flat sheet configuration in a previous project (CO_2 permeance of 1.1E-4 scc/(cm^2 s cm Hg) and a CO_2/O_2 selectivity of 1410), we designed a system that has volume of 2.04 ft^3/crew. The system has a power consumption requirement of 84.2 watts/crew if pump efficiencies and heat losses are not considered and 213.7 watts/crew if pump efficiencies and heat losses equivalent to those in the CDRA are factored in. The system is capable of delivering a continuous flow of dry, concentrated CO_2 to the Sabatier reactor without requiring an accumulator or compressor for storage. Finally, the concentrations of both N_2 and O_2 in the Sabatier feed are both less than 1% by volume.

Acknowledgments

The authors are grateful to Robyn Gatens for providing funding for this work under Phase III Contract # NNJ15HD38P. We also are very grateful to our contract monitor, Cinda Chullen, for her active involvement throughout the course of this project. Finally we would like to thank Jim Knox and Jeff Sweterlitsch for their comments and suggestions.

References

[1] Knox, J.C., H. Gauto, R. Gostowski, D. Watson, R. Bush, L. Miller, C. Stanley, and J. Thomas (2014). "Development of Carbon Dioxide Removal Systems for Advanced Exploration Systems 2013-2014," Paper No. ICES-2014-160, 44th International Conference on Environmental Systems, Tucson, AZ.

[2] Schunk, R.G., R.M. Bagdigian, R.L. Carrasquillo, K.Y. Ogle, and P.O. Wieland (1989). "Space station ECLSS simplified integrated test(Final Report)." NASA TM-100363.

[3] Murdock, K. (2010). "Integrated Evaluation of Closed Loop Air Revitalization System Components." NASA/CR-2010-216451.

[4] Wasserschieid, P. and T. Welton, *Ionic Liquids in Synthesis*, Wiley-VCH Verlag GmbH & Co. KgaA, Weinheim (2008).

[5] Wickham, D.T., K.J. Gleason, and S. Cowley (2014a) Advanced Supported Liquid Membranes for CO_2 Control in EVA Applications, SBIR Phase II Final Report for NASA contract #NNX12CA65C, NASA – Johnson Space Center ,Houston, TX.

[6] Wickham, D.T., K J. Gleason, J. R. Engel, S. W. Cowley, and C. Chullen (2014b). "Advanced Supported Liquid Membranes for Carbon Dioxide Control in Extravehicular Activity Applications", Paper No. ICES-2014-231, 44th International Conference on Environmental Systems, Tucson, AZ.

[7] Culligan (2016). Accessed at http://www.culligan.com.ar/seminariodiadelagua/ Descargas/ presentation2-membranetechnology.pdf

[8] Peters, M.S., K.D. Timmerhaus, R.E. West (2003). "Plant Design Economics for Chemical Engineers", Fifth Edition, McGraw-Hill Higher Education, New York.

[9] Wang, Y. and M. D. LeVan (2009). "Adsorption equilibrium of carbon dioxide and water vapor on zeolites 5A and 13X and silica gel: pure components." Journal of Chemical & Engineering Data 54.10, pp 2839-2844.

[10] Avallone, E.A, and T. Baumeister (1976). Marks' Standard Handbook for Mechanical Engineers, Tenth Edition, McGraw-Hill, New York.